*Geophys. J. Int.* (2002) **150,** 737–752

# Palaeomagnetic and rock-magnetic studies of Cretaceous rocks in the Gongju Basin, Korea: implication of clockwise rotation

Seong-Jae Doh,[1] Wonnyon Kim,[1] Dongwoo Suk,[2] Yong-Hee Park[1] and Daekyo Cheong[3]

[1] *Department of Earth and Environmental Sciences, Korea University, Seoul,* 136-701, *Korea. E-mail: sjdoh@korea.ac.kr*
[2] *Department of Earth and Marine Sciences, Hanyang University, Ansan,* 425-791, *Korea*
[3] *Division of Earth Sciences, Kangwon National University, Chuncheon,* 200-701, *Korea*

Accepted 2002 March 18. Received 2002 March 4; in original form 2001 June 5

## SUMMARY

Palaeomagnetic and rock-magnetic studies have been carried out for Cretaceous non-marine sedimentary rocks (Gongju Group) and volcanic rocks in the Gongju Basin, located along the northern boundary of the Ogcheon Belt, Korea. K–Ar age dating for the volcanic rocks was also performed. It is found that the Gongju Group was remagnetised during the tilting of the strata with the characteristic remanent magnetisation (ChRM) direction of $D/I = 23.9^\circ/50.6^\circ$ ($k = 95.5$, $\alpha_{95} = 3.9^\circ$) at 30 per cent untilting of the strata with a maximum value of precision parameter ($k$), while the volcanic rocks are revealed to acquire primary remanence with the direction of $D/I = 204.2^\circ/-43.8^\circ$ ($k = 36.6$, $\alpha_{95} = 8.6^\circ$) after the tilt-correction. The K–Ar ages of the volcanic rocks range from 81.8 ± 2.4 to 73.5 ± 2.2 Ma, corresponding to the Campanian stage of the Late Cretaceous. Electron microscope observations of samples from the Gongju Group show authigenic iron-oxide minerals of various sizes distributed along the cleavage of chlorite and in the pore spaces, indicating that the strata acquired the chemical remanent magnetisation due to the formation of secondary magnetic minerals under the influence of fluids. The palaeomagnetic pole positions are at Lat./Long. = 69.6°N/224.3°E ($dp = 3.5^\circ$, $dm = 5.2^\circ$) calculated for the 30 per cent tilt-corrected direction of the Gongju Group and at Lat./Long. = 67.2°N/235.3°E ($A_{95} = 8.9^\circ$) for the volcanic rocks. Based on the results of this study, it is interpreted that the volcanic rocks acquired the primary magnetisation almost at the same time as the remagnetisation of the Gongju Group in the Late Cretaceous. Comparisons of Cretaceous palaeomagnetic poles from the Korean Peninsula with those from Eurasia implies that the Korean Peninsula underwent clockwise rotation of $21.2^\circ \pm 5.3^\circ$ for the middle Early Cretaceous, $12.6^\circ \pm 5.4^\circ$ for the late Early Cretaceous, and $7.1^\circ \pm 9.8^\circ$ for the Late Cretaceous with respect to Eurasia, due to the sinistral motion of the Tan-Lu Fault.

**Key words:** Cretaceous, Gongju Basin, Korea, palaeomagnetism, remagnetisation, rotation.

## 1 INTRODUCTION

The primary object of palaeomagnetic study is to obtain directions of the past geomagnetic field recorded in rocks. These fossil geomagnetic field directions with respect to that of the present day field make it possible to solve various geological problems, such as age estimation of rocks and deciphering tectonic history based on the reconstruction of major and micro plates through the geological time. Such palaeomagnetic characterisation of the Cretaceous rocks in the Korean Peninsula has been successfully carried out primarily for the Gyeongsang Basin in the southeastern part of the Korean Peninsula (Min *et al.* 1982; Otofuji *et al.* 1983, 1986; Kim & Jeong 1986; Lee *et al.* 1987; Kim & Kim 1991; Doh *et al.* 1994; Doh & Kim 1994; Zhao *et al.* 1999), for which the palaeomagnetic directions and pole positions are well established. However, only a few palaeomagnetic studies were performed for the Cretaceous basins outside the Gyeongsang Basin. Thus detailed palaeomagnetic investigations are still required for the Cretaceous basins other than the Gyeongsang Basin to verify the palaeomagnetic characteristics of the Cretaceous rocks.

Along the boundary between the Gyeonggi Massif and the Ogcheon Belt (Fig. 1), there are three relatively small Cretaceous basins of a similar tectonic origin on the Gyeonggi Massif side, the Eumseong, Gongju, and Gapcheon basins. Only two palaeomagnetic studies have been carried out for the rocks from these Cretaceous basins. A palaeomagnetic study of the Eumseong, Gongju, and Gapcheon basins was reported by Lee *et al.* (1992), for which a very limited number of samples was collected: 5 samples from 1 site for the Eumseong Basin, 27 samples from 4 sites for the Gongju Basin, and 18 samples from 2 sites for the Gapcheon Basin, and the palaeomagnetic directions showed large dispersion. These palaeomagnetic results, therefore, cannot be considered as the representative

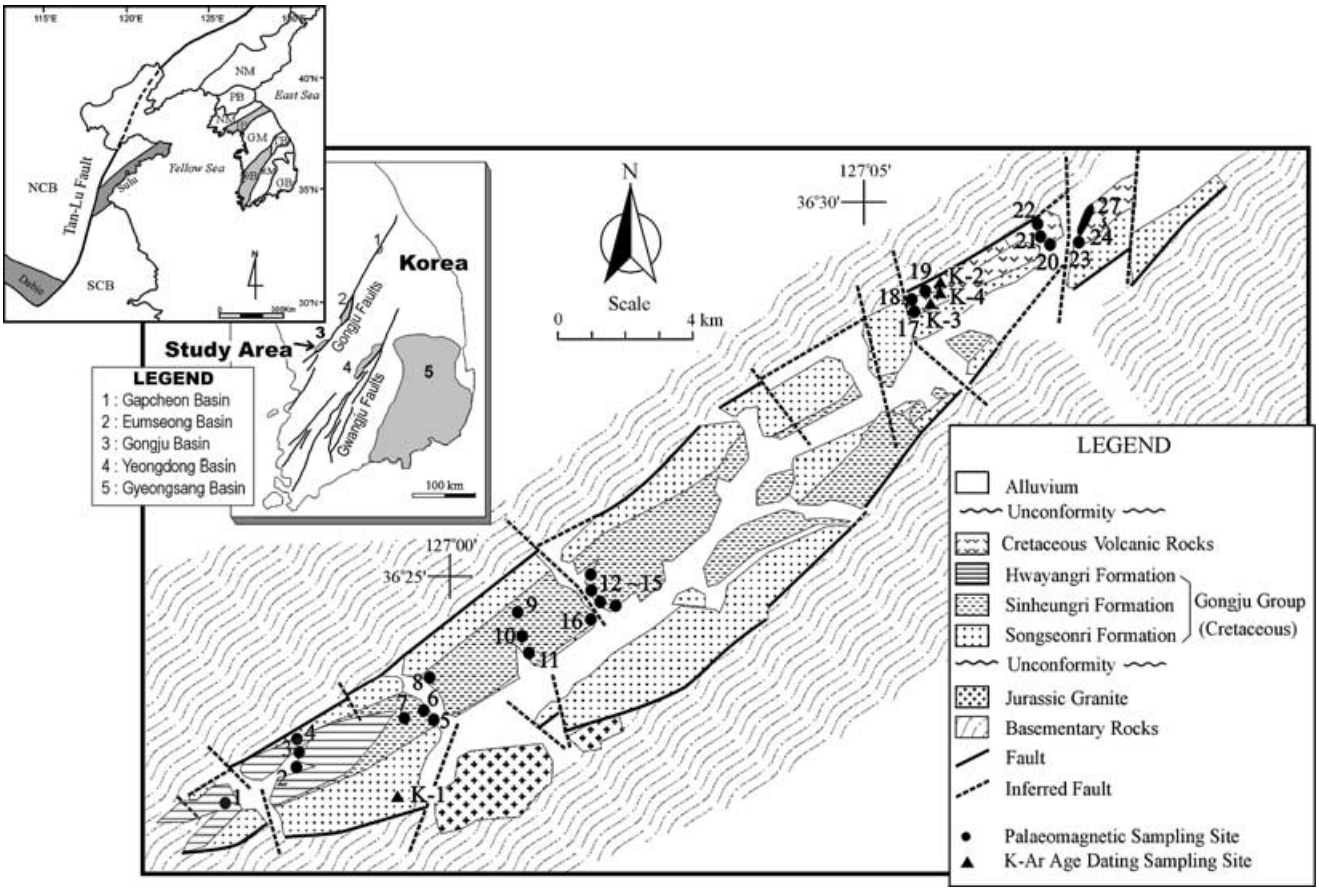


**Figure 1.** Tectonic setting of East Asia and distribution of the Cretaceous basins, and Geological map of the Gongju Basin showing locations of sampling sites. NCB: North China Block; SCB: South China Block; NM: Nangrim Massif; PB: Pyeongnam Basin; IB: Imjingang Belt; GM: Gyeonggi Massif; OB: Ogcheon Belt; TB: Taebaeksan Basin; RM: Ryeongnam Massif; GB: Gyeongsang Basin.

directions for each basin. The other study was of the Eumseong Basin for which palaeomagnetic results were obtained by measuring 765 samples from 41 sites (Doh *et al.* 1999). However, they reported that the characteristic remanent directions of the rocks from the Eumseong Basin were remagnetised. Because these two studies did not yield characteristic directions for the Cretaceous Period, it is important to know the representative palaeomagnetic direction of the Cretaceous basins within the Gyeonggi Massif. Furthermore, some workers reported that the Korean Peninsula underwent vertical-axis clockwise rotation with respect to China during the Cretaceous Period (Otofuji *et al.* 1986; Lee *et al.* 1987; Ma *et al.* 1993; Doh & Piper 1994; Zhao *et al.* 1999; Uno & Chang 2000). The sinistral motion of the Tan-Lu Fault (Ma *et al.* 1993; Doh & Piper 1994; Uno & Chang 2000) or Kula–Eurasia plate convergence (Zhao *et al.* 1999) have been suggested as possible causes of rotation. However the time, scale, and magnitude of rotations are still questionable. Palaeomagnetic and rock-magnetic studies with K–Ar age determinations have been carried out for the Cretaceous rocks in the Gongju Basin, in order to find out the palaeomagnetic direction and pole position, to give information on magnetisation processes in relation to sedimentation and volcanic activity, and to understand tectonic settings since the Cretaceous.

## 2 GEOLOGICAL SETTING

The Gongju Basin, about 6 km wide and 24 km long, is situated near the boundary between the Ogcheon Belt and the Gyeonggi Massif (Lat. = 36°25′, Long. = 127°03′) (Fig. 1). The basement structure was initiated as a ductile shear zone followed by brittle shear deformation at the time of the Jurassic Daebo Orogeny (Lee 1990), and resulted in a half-graben formed by the extensive crustal upheaval during the Cretaceous Period (Lee 1988; Choi 1999). The shear zone became a secondary sinistral strike-slip fault zone at the surface forming the Gongju Basin, which was filled with Cretaceous non-marine sedimentary rocks (Gongju Group), and volcanic rocks in the northeastern part of the basin.

The Gongju Group is composed of three formations classified on the basis of their lithological characteristics: the Songseonri Formation, the Sinheungri Formation and the Hwayangri Formation in ascending order of age (Lee 1990). The Songseonri Formation, consisting mainly of pebbly sandstone and conglomerate, is not included in this study because the lithology is not adequate for a palaeomagnetic study. The Sinheungri Formation, conformably overlies the Songseonri Formation, is mainly composed of purplish siltstone and shale (red bed) with strike direction of about N30° ∼ 80°E and dip of 30° ∼ 75°NW or SE. Around the town of Sinheungri, the Sinheungri Formation shows ripple-marks and mud cracks, indicating that the formation had been exposed to the air and did not experience any deformational processes (Lee 1990). The Hwayangri Formation, mainly composed of lacustrine-type black shale, is located in the southwestern part of the Gongju Basin. The Hwayangri Formation shows about N40°E strike and 50°NW dip. Plant fossils, *Frenelopsis species*, reported from the Hwayangri Formation (Song *et al.* 1991) are correlated with those found in the upper Hayang

Group (e.g. Sagok and Chunsan formations) in the Gyeongsang Basin (Choi 1999), indicating that the Gongju Group was formed during the late Early Cretaceous. The volcanic rocks, which are correlated with the Late Cretaceous Yucheon Group in the Gyeongsang Basin (Choi 1999), are exposed in the northeastern part of the study area, and show strike of about N60° ∼ 80°E and steep dip angle of about 70°NW. The attitudes of some volcanic rocks, which do not show bedding structure, were measured from the adjacent sedimentary strata.

## 3 EXPERIMENTAL METHODS

The samples were cored with a gasoline-powered portable rock drill and oriented with a Brunton compass. The locations of sampling sites are shown in Fig. 1. A total of 331 samples from 27 sites was collected: 4 sites from the Hwayangri Formation, 12 sites from the Sinheungri Formation, and 11 sites from the volcanic rocks. The 25 mm diameter cored samples were cut into 22 mm long cylinders in the laboratory. During the palaeomagnetic experiments, all samples were stored in mu-metal shield boxes to prevent subsequent acquisition of magnetisation by the external magnetic field such as the Earth's field.

To determine a proper demagnetising method, four pilot samples were selected from each site and were treated by alternating field (AF) and thermal demagnetisations, and the remaining samples were treated using the proper demagnetising method determined by the pilot sample treatments. AF demagnetisation was performed at the field strength of 5 ∼ 30 mT with 5 mT intervals, 30 ∼ 60 mT with 10 mT intervals, and 60 ∼ 100 mT with 20 mT intervals using a Schonstedt tumbling specimen demagnetiser (model GSD-5). Thermal demagnetisation was performed at 100, 200, 300, 350, 400, 450, 500°C and for temperature range of 520 ∼ 700°C with 20°C intervals using an ASC thermal demagnetiser (model TD-48). The palaeomagnetic direction of the samples for each demagnetisation step was measured using a Molspin spinner magnetometer and a 2G cryogenic magnetometer (model 760R). To monitor possible chemical changes of magnetic materials during heating, magnetic susceptibility was measured at each step of the thermal demagnetisation using a Bartington magnetic susceptibility meter (model MS2). The palaeomagnetic data obtained from all samples were plotted in the orthogonal vector diagram (Zijderveld 1967) and the ChRM direction of each sample was determined by the principal component analysis (PCA) with anchored line fit method (Kirschvink 1980) using at least three or more consecutive data points.

To reveal the magnetic carriers, isothermal remanent magnetisation (IRM) acquisition experiments for representative samples from each site were performed using ASC Impulse Magnetisers (model IM-10 and IM-10–30). In these experiments, a maximum field of 2.5 T was used for the acquisition of saturation isothermal remanent magnetisation (SIRM). Hysteresis parameters were measured with a Molspin vibrating sample magnetometer (model VSM Nuvo) for selected samples. To confirm the size, shape and composition of magnetic carriers, electron microscope observations were performed for representative samples.

Volcanic rock samples, occurring as a dyke (K-1) and volcanic flows (K-2, K-3 and K-4) covering sedimentary rocks, were collected from the fresh outcrops for the K–Ar age determinations (Fig. 1). The samples were crushed first into 150 ∼ 75 $\mu$m size to remove phenocrysts (usually plagioclase) to prevent an excess Ar problem. Potassium analyses were carried out by an atomic absorption spectrophotometer (model Unicam 989) using a 2000 ppm Cs buffer. Samples were decomposed with mixed acids ($HF:HNO_3:HClO_4 = 4:4:1$) in a pressurized Teflon bomb. Multiple runs of a chemical standard (RGM-1) indicate that the accuracy of this method was within 3 per cent. An average value of duplicate runs was used in age calculations. Argon was analysed on a 90° and 54 cm radius sector type mass spectrometer (model VG5400) with a double collector system (high Faraday collector and electron multiplier) operated at an accelerating potential of 4.5 kV and trap current of 200 $\mu$A using an isotopic dilution method and an $Ar^{38}$ spike. Calibration of the $Ar^{38}$ spike is accurate to within about 1 per cent. Mass discrimination was checked with atmospheric argon once each day. Calculations of ages and error are made following the method described by Nagao *et al.* (1996). The use of standard analyses before and after argon analyses of a sample batch ensured that the argon analyses were accurate to within 2 per cent, the error of each age determination.

## 4 PALAEOMAGNETIC RESULTS AND K–Ar AGES

### 4.1 The Gongju Group

Typical examples of AF and thermal demagnetisation behaviour of the Hwayangri Formation are shown in Figs 2(a) and (b). The characteristic components of most samples are isolated above 20 mT or 500°C, while the low coercivity and/or low temperature components can be removed in the initial demagnetisation steps of AF demagnetisation at about 10 ∼ 20 mT and/or thermal demagnetisation level of about 200 ∼ 500°C. The mean direction (declination/inclination, $D/I$) of ChRMs from the Hwayangri Formation is $D/I = 12.6°/52.9°$ ($k = 172.0$, $\alpha_{95} = 7.0°$) before tilt correction and $D/I = 58.4°/42.1°$ ($k = 202.4$, $\alpha_{95} = 6.5°$) after tilt correction (Table 1). Although the in situ directions are slightly more dispersed than tilt corrected directions (Fig. 3a), subsequent stepwise unfolding test yields the maximum clustering at 50 per cent unfolding of the formation with the characteristic direction of $D/I = 39.0°/51.5°$ ($k = 517.1$, $\alpha_{95} = 4.0°$).

For the Sinheungri Formation, the demagnetisation experiments of the pilot samples reveal that the thermal demagnetisation method is more effective to isolate the characteristic component, while the AF demagnetisation cannot remove the remanent magnetisation successfully even at the field strength of 100 mT. Therefore, the thermal demagnetisation method was applied to all samples from the Sinheungri Formation to isolate the ChRMs. Typical demagnetisation behaviour is shown in Fig. 2(c). The secondary components are easily removed at about 300 ∼ 500°C, and the stable components appear up to 680°C heating steps. Site KJ9 is excluded from the calculated mean because it showed a mean direction anomalous with respect to the mean of the remaining sites. The mean direction of ChRMs from the Sinheungri Formation is $D/I = 40.0°/57.5°$ ($k = 37.6$, $\alpha_{95} = 7.5°$) before tilt correction and $D/I = 4.8°/21.9°$ ($k = 66.0$, $\alpha_{95} = 5.7°$) after tilt correction. Even though the in situ directions are more dispersed than tilt corrected directions (Fig. 3b), the stepwise unfolding test reveals the maximum clustering at 60 per cent unfolding with $D/I = 11.8°/38.7°$ ($k = 118.3$, $\alpha_{95} = 4.2°$).

The mean direction of the Gongju Group is $D/I = 32.0°/56.9°$ ($k = 35.1$, $\alpha_{95} = 6.5°$) before tilt correction, and $D/I = 16.2°/29.1°$ ($k = 11.7$, $\alpha_{95} = 11.7°$) after tilt correction. The tilt corrected directions of the Gongju Group are more dispersed than the in situ directions (Table 1 and Fig. 3c), indicating that the ChRMs are not primary. The stepwise unfolding test shows that the maximum clustering of ChRM directions occurs at 30 per cent unfolding (Fig. 4), at which the palaeomagnetic direction is $D/I = 23.9°/50.6°$

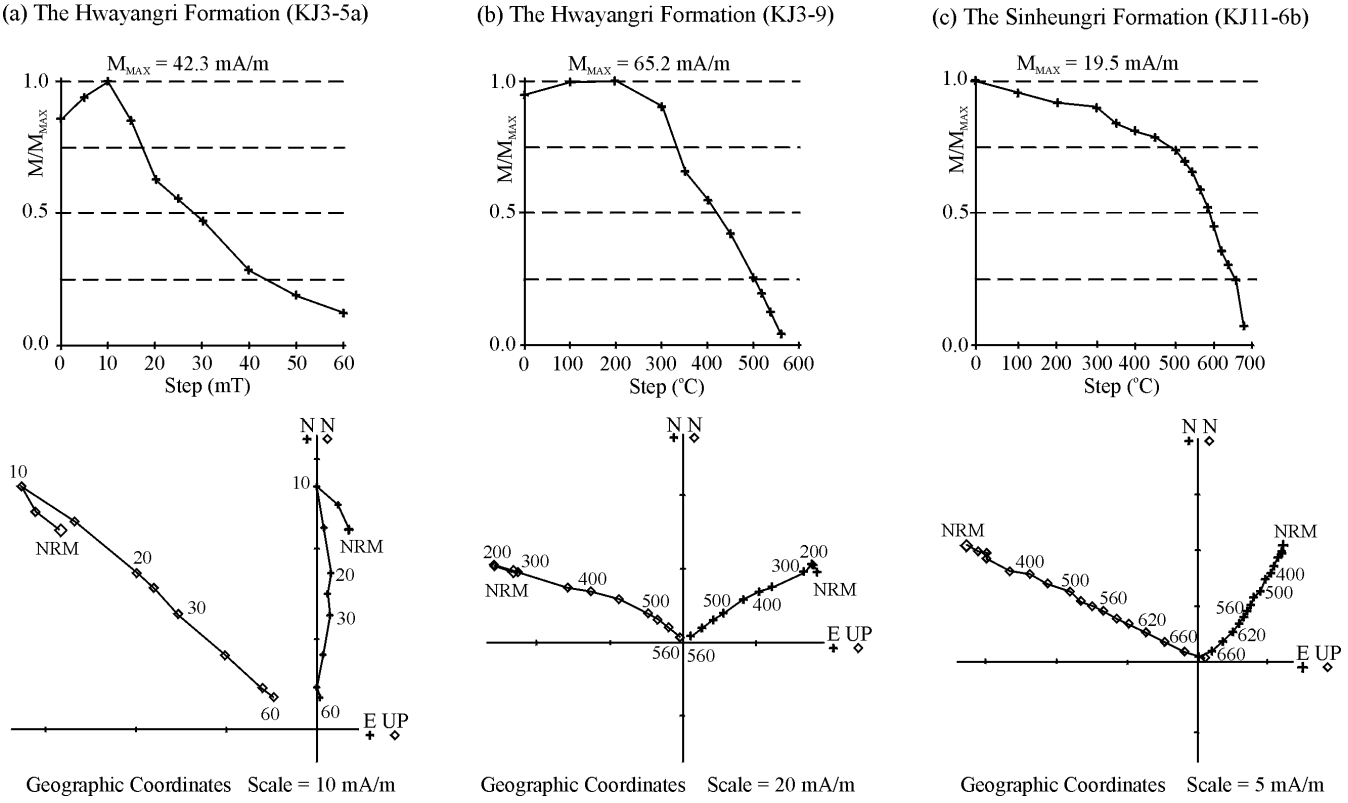


**Figure 2.** Typical AF (a) and thermal (b and c) demagnetisation results of the Hwayangri and Sinheungri formations. Normalized intensity curves and Zijderveld diagrams are shown.

($k = 95.5, \alpha_{95} = 3.9°$). In addition, the parameter estimating fold test (Watson & Enkin 1993) gives the maximum $k$ value at 34.9 per cent untilting, with 95 per cent confidence interval of 33.0 $\sim$ 37.0 per cent untilting when the number of parametric resampling is 1000. These results indicate that the ChRMs of the Gongju Group are remagnetised components.

### 4.2 Volcanic rocks

Palaeomagnetic results from the volcanic rocks can be classified into two groups according to demagnetisation behaviours. The magnetic intensity drastically decreases near 580°C for magnetite-dominant samples from sites KJ19, KJ22, KJ25, KJ26, and KJ27 and at around 680°C for haematite-dominant samples from sites KJ17, KJ18, KJ20, KJ21, KJ23 and KJ24 (Fig. 5). For the magnetite-dominant samples, secondary viscous components can be erased at about 450°C, and characteristic components are isolated in the temperature range of 450 $\sim$ 580°C (Fig. 5a). It turned out that the thermal demagnetisation method is more effective to isolate the ChRM directions for the haematite-dominant samples, for which secondary viscous components are removed up to 500°C and stable components are isolated at demagnetisation levels between 500°C and 680°C (Fig. 5b).

The mean direction of the ChRMs from the volcanic rocks, regardless of the type of demagnetisation behaviour, is $D/I = 276.0°/-47.9°$ ($k = 3.0$, $\alpha_{95} = 35.6°$) before tilt correction and $D/I = 204.2°/-43.8°$ ($k = 36.6, \alpha_{95} = 8.6°$) after tilt correction. Sites KJ23 and KJ24 are not included in calculation of the mean direction, because the NRM intensities of samples from these sites are too weak (less than 1 mA m$^{-1}$) and the directions of ChRM have unacceptable values of the precision parameter and confidence limit (KJ23: $k = 2.0$ and $\alpha_{95} = 55.5°$; KJ24: $k = 14.9$ and $\alpha_{95} = 23.0°$) (Table 2). In situ directions are more dispersed than tilt corrected directions (Fig. 6). The data also passed the reversal test based on the fact that the reversed components are statistically the same directions as normal components at the 95 per cent confidence level. The stepwise unfolding test shows that the maximum clustering of ChRM directions occurs at 100 per cent unfolding (Fig. 7). These results indicate that the ChRMs of the volcanic rocks have been acquired during or soon after the formation of the volcanic rocks.

The K–Ar ages of the volcanic rocks range from 81.8 $\pm$ 2.4 to 73.5 $\pm$ 2.2 Ma. The maximum age of 81.8 $\pm$ 2.4 Ma is obtained from a dyke intruded in the Songseonri Formation (K-1) and ages of samples from volcanic flows fall into relatively short time span: K-2, K-3 and K-4 are 73.5 $\pm$ 2.2, 80.3 $\pm$ 2.4 and 76.8 $\pm$ 2.3 Ma respectively (Table 3). The volcanic rocks are dated as Campanian stage (83.5 $\pm$ 0.5 $\sim$ 71.3 $\pm$ 0.5 Ma, Gradstein *et al.* 1994) of the Late Cretaceous. The presence of reversals in the volcanic rocks, in accordance of Campanian polarity variations, confirms the age determinations of the rocks.

## 5 ROCK MAGNETIC RESULTS

In the Gongju Group, there is distinctive IRM behaviour between the two formations. In general, samples from the Hwayangri Formation show the rapid acquisition of IRM in the fields of less than 100 mT and reaching more than 90 per cent saturation below 300 mT (Fig. 8a), indicating that a ferrimagnetic mineral such as magnetite is a major contributor to the magnetisation. In the case of a sample KJ1-6a, it shows a sharp increase of IRM up to 300 mT by

**Table 1.** Palaeomagnetic results of the Gongju Group.

| Formation | Site | n | Site | | Dg (°) | Ig (°) | Ds (°) | Is (°) | $k$ | $\alpha_{95}$ (°) | VGP | | $dp$ (°) | $dm$ (°) |
|---|---|---|---|---|---|---|---|---|---|---|---|---|---|---|
| | | | Long. (°E) | Lat. (°N) | | | | | | | Long. (°E) | Lat. (°N) | | |
| Hwayangri Formation | KJ1 | 11 | 126.95 | 36.35 | 10.7 | 59.9 | 54.9 | 37.5 | 36.8 | 7.6 | 219.2 | 40.1 | 5.3 | 8.9 |
| | KJ2 | 13 | 126.97 | 36.37 | 10.4 | 53.8 | 66.6 | 41.2 | 64.6 | 5.0 | 209.7 | 32.1 | 3.7 | 6.1 |
| | KJ3 | 17 | 126.97 | 36.37 | 9.8 | 51.0 | 54.7 | 46.9 | 278.3 | 2.2 | 210.8 | 43.6 | 1.8 | 2.8 |
| | KJ4 | 13 | 126.97 | 36.38 | 18.5 | 46.5 | 57.4 | 42.5 | 124.1 | 3.7 | 213.6 | 39.9 | 2.8 | 4.6 |
| | Mean | 4/4 | | | 12.6 | 52.9 | | | 172.0 | 7.0 | | | | $K = 190.3$ |
| | | | | | | | 58.4 | 42.1 | 202.4 | 6.5 | 213.3 | 39.0 | | $A_{95} = 6.7$ |
| Sinheungri Formation | KJ5 | 17 | 127.00 | 36.38 | 60.1 | 49.0 | 6.2 | 13.8 | 61.7 | 4.6 | 294.6 | 60.1 | 2.4 | 4.7 |
| | KJ6 | 18 | 127.00 | 36.38 | 48.3 | 56.0 | 6.1 | 7.8 | 258.4 | 2.2 | 295.8 | 57.1 | 1.1 | 2.2 |
| | KJ7 | 18 | 126.98 | 36.38 | 50.7 | 45.1 | 11.2 | 21.2 | 107.7 | 3.3 | 282.5 | 62.7 | 1.8 | 3.5 |
| | KJ8 | 17 | 126.98 | 36.38 | 4.0 | 58.3 | 10.4 | 25.0 | 157.0 | 2.9 | 282.5 | 64.9 | 1.7 | 3.1 |
| | KJ9* | 10 | 127.02 | 36.40 | 359.8 | 27.4 | 40.7 | 35.6 | 148.1 | 4.5 | 235.1 | 48.9 | 2.8 | 5.0 |
| | KJ10 | 16 | 127.02 | 36.38 | 43.3 | 52.8 | 358.8 | 25.1 | 270.4 | 2.4 | 310.0 | 66.8 | 1.4 | 2.6 |
| | KJ11 | 15 | 127.02 | 36.38 | 45.2 | 62.7 | 6.1 | 13.6 | 193.9 | 2.8 | 294.8 | 60.0 | 1.5 | 2.9 |
| | KJ12 | 19 | 127.03 | 36.40 | 51.5 | 37.2 | 10.7 | 40.2 | 81.2 | 3.9 | 269.6 | 73.6 | 2.8 | 4.7 |
| | KJ13 | 12 | 127.03 | 36.40 | 30.2 | 61.6 | 7.2 | 23.3 | 484.8 | 2.1 | 290.2 | 64.9 | 1.2 | 2.2 |
| | KJ14 | 20 | 127.03 | 36.40 | 19.3 | 64.0 | 351.1 | 22.7 | 208.1 | 2.4 | 327.3 | 64.1 | 1.4 | 2.5 |
| | KJ15 | 14 | 127.03 | 36.40 | 23.5 | 68.3 | 0.6 | 22.4 | 91.4 | 4.4 | 305.6 | 65.2 | 2.5 | 4.4 |
| | KJ16 | 9 | 127.03 | 36.38 | 37.2 | 66.4 | 5.2 | 24.4 | 181.9 | 4.1 | 294.5 | 65.9 | 2.4 | 4.4 |
| | Mean | 11/12 | | | 40.0 | 57.5 | | | 37.6 | 7.5 | | | | $K = 113.9$ |
| | | | | | | | 4.8 | 21.9 | 66.0 | 5.7 | 295.8 | 64.8 | | $A_{95} = 4.3$ |
| Gongju Group | Mean | 15/16 | 0% untilting | | 32.0 | 56.9 | | | 35.1 | 6.5 | 203.7 | 65.2 | | $K = 22.1$ |
| | | | | | | | | | | | | | | $A_{95} = 8.3$ |
| | | | 100% untilting | | | | 16.2 | 29.1 | 11.7 | 11.7 | | | | |
| | | | 30% untilting | | | | 23.9 | 50.6 | 95.5 | 3.9 | 224.3 | 69.6 | 3.5 | 5.2 |

n: number of samples; Dg and Ig: declination and inclination in geographic coordinates; Ds and Is: declination and inclination in stratigraphic coordinates; $k$: Fisherian precision parameter; $\alpha_{95}$: radius of cone of 95 per cent confidence interval; VGP: virtual geomagnetic pole; $dp$: the semi axis of the confidence ellipse along the great-circle path from site to pole; $dm$: the semi axis of the confidence ellipse perpendicular to that great-circle path; $K$: the best-estimate of the precision parameter $k$ for the observed distribution of site-mean VGPs; $A_{95}$: the radius of the 95 per cent confidence circle about the calculated mean pole.*: KJ9 is excluded from the calculation of formation mean direction.

the contribution of a ferrimagnetic mineral, followed by the gradual acquisition of additional IRM in stronger magnetising fields. IRM acquired in the field higher than 300 mT is due to the presence of a high coercive force mineral such as haematite. The IRM acquisition curves of the Sinheungri Formation show a gradual acquisition of IRM up to the maximum magnetising field of 2.5 T, indicating that a canted antiferromagnetic mineral is a major contributor to the magnetisation (Fig. 8b). The two distinctive IRM acquisition patterns were also observed in samples from the volcanic rocks. The ferrimagnetic-mineral-dominant pattern was observed in samples from sites KJ22, KJ25, KJ26 and KJ27 (Fig. 8c), and the canted antiferromagnetic-mineral-dominant pattern was observed in samples from sites KJ18, KJ21, KJ23 and KJ24 (Fig. 8d).

Representative samples were selected for the measurement of the hysteresis parameters. The hysteresis parameters (saturation remanence, $M_{rs}$; saturation magnetisation, $M_s$; coercivity of remanence, $H_{cr}$; coercive force, $H_c$) are listed in Table 4. Samples from the Hwayangri Formation reveal that the values of the hysteresis parameters ($H_{cr} = 47.49 \sim 78.19$ mT, $M_{rs} = 0.70 \sim 14.08$ $\mu$Am$^2$ and $M_s = 66.88 \sim 115.96$ $\mu$Am$^2$) are comparable to those of a ferrimagnetic mineral, while samples from the Sinheungri Formation have $H_{cr}$ (52.34 ~ 588.10 mT), $M_{rs}$ (1.38 ~ 4.93 $\mu$Am$^2$) and $M_s$ (19.65 ~ 73.61 $\mu$Am$^2$) values similar to those of a canted antiferromagnetic mineral such as haematite. In the volcanic rocks, both magnetite-rich samples with relatively low $H_{cr}$ (28.80 ~ 108.77 mT), relatively high $M_{rs}$ (5.08 ~ 103.71 $\mu$Am$^2$) and $M_s$ (54.56 ~ 301.07 mT) and haematite-rich samples having relatively high $H_{cr}$ (173.81 ~ 676.63mT), relatively low $M_{rs}$ (1.29 ~ 12.62 $\mu$Am$^2$) and $M_s$ (29.33 ~ 78.03 $\mu$Am$^2$) were observed. These results of the magnetic hysteresis measurements are in good agreement with those of the IRM acquisition and demagnetisation experiments. The ratios of hysteresis parameters, $H_{cr}/H_c$ and $M_{rs}/M_s$, were used to diagnose the domain state of magnetic minerals (Day *et al.* 1977). From the diagram of the $M_{rs}/M_s$ versus $H_{cr}/H_c$, it is revealed that the magnetite-dominant samples are mostly in pseudo-single domain (PSD) state with some in multi-domain (MD) or superparamagnetic (SPM) state (Fig. 9).

## 6 ELECTRON MICROSCOPE OBSERVATIONS

Electron microscope observations were carried out to characterise shape, size and composition of magnetic carriers and adjacent minerals. In order to identify iron-oxide and accompanying minerals, compositional analyses using an energy dispersive analysis (EDA) system were performed. Although observations of the samples from the Hwayangri Formation cannot reveal any characteristics of magnetic carriers because the size of magnetic carriers is too small to be detected during the scanning of the samples at the magnification of 2000, it may suggest that the magnetic carriers in these samples are in PSD or SD state. The samples from the Sinheungri Formation

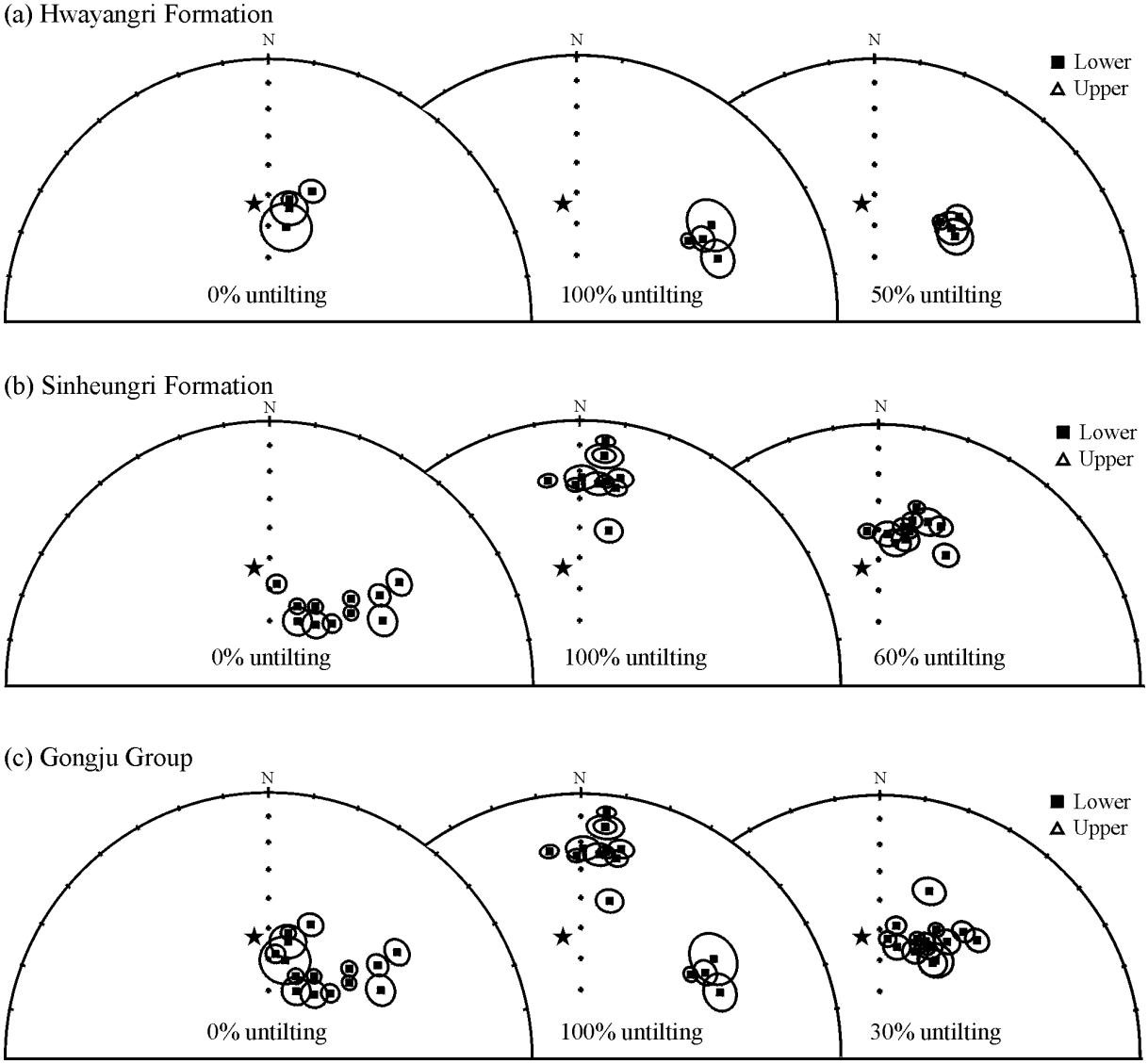


**Figure 3.** Equal area projections of the site mean directions with 95 per cent confidence circle of the (a) Hwayangri Formation, (b) Sinheungri Formation and (c) Gongju Group. (star: present field direction: $D/I = 352.6^\circ/52.9^\circ$).

show abundant occurrences of iron-oxide minerals of various sizes (Fig. 10). Fig. 10(a) shows that a large iron-oxide grain, about 10 $\mu$m in length, authigenically filled in a void surrounded by minerals such as quartz, K-feldspar, calcite and chlorite. Fig. 10(b) shows a large void-filling iron-oxide mineral at the centre and submicron size needle shaped iron-oxide minerals within the cleavage of chlorite in the upper-right corner. Aggregates of iron-oxide grains possibly precipitated around the chlorite grain boundaries are shown in Fig. 10(c). Fig. 10(d) is the image of small iron-oxide grains of submicron to 2 $\mu$m in length precipitated in the pore spaces. Shape, composition and relationship to adjacent minerals of iron-oxides in Figs 10(a)–(d) suggest that they were formed authigenically under the influence of Fe-bearing fluids, such as meteoric and/or formational water.

The most frequently observed magnetic minerals in samples from the volcanic rocks are iron-oxide minerals with small amount of Ti and, less frequently, with ilmenite lamellae. Fe-Ti oxides that originally crystallize from igneous melts are referred to as primary magnetic minerals. In Fig. 10(e), anhedral to subhedral iron-oxide grains of about $0.1 \sim 7$ $\mu$m in length are shown. These Ti-containing iron-oxides without ilmenite lamellae within clinopyroxene indicate lack of exsolution of ulvöspinel and/or ilmenite. Such single-phase titaniferous iron-oxides may form only at high temperatures that exceed the temperature of the magnetite-ulvöspinel solvus, with rapid cooling from that level (Van der Voo *et al.* 1993). Also iron-oxides with ilmenite lamellae in plagioclase grains are interpreted as a primary magnetic mineral in origin (Fig. 10f).

## 7 DISCUSSION

### 7.1 Timing of remagnetisation of the Gongju Group

The *in situ* mean direction of the Gongju Group is statistically better than the tilt corrected direction, although the Hwayangri and Sinheungri formations, individual formations comprising the Gongju Group, yield opposite results (Table 1). The mean directions of the Hwayangri and Sinheungri formations show better clustered directions at 50 per cent and 60 per cent unfolding, respectively,

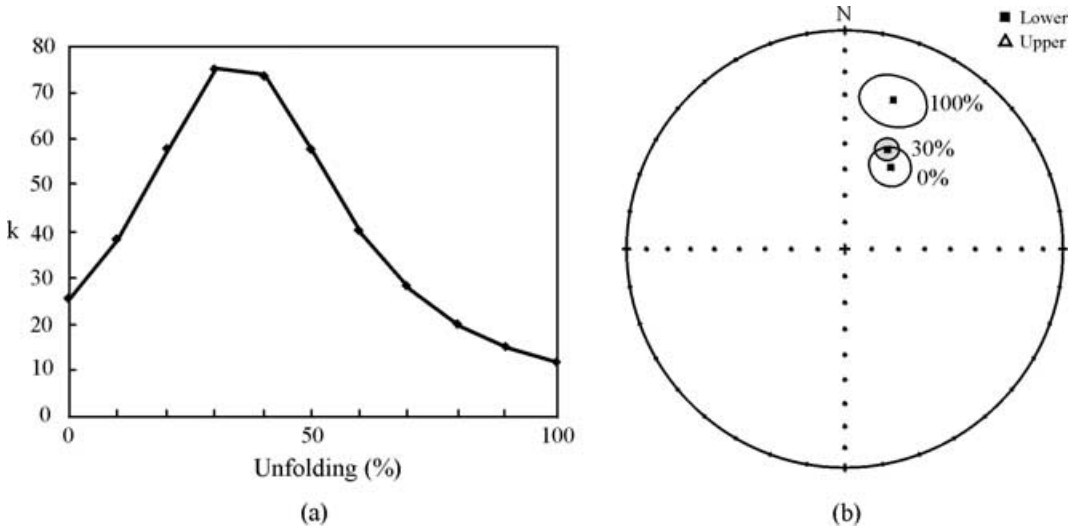


**Figure 4.** Results of the stepwise unfolding test of the Gongju Group. (a) Plots of Fisher's precision parameter ($k$) versus percent unfolding and (b) palaeomagnetic directions at 0 per cent, 30 per cent and 100 per cent unfolding are shown.

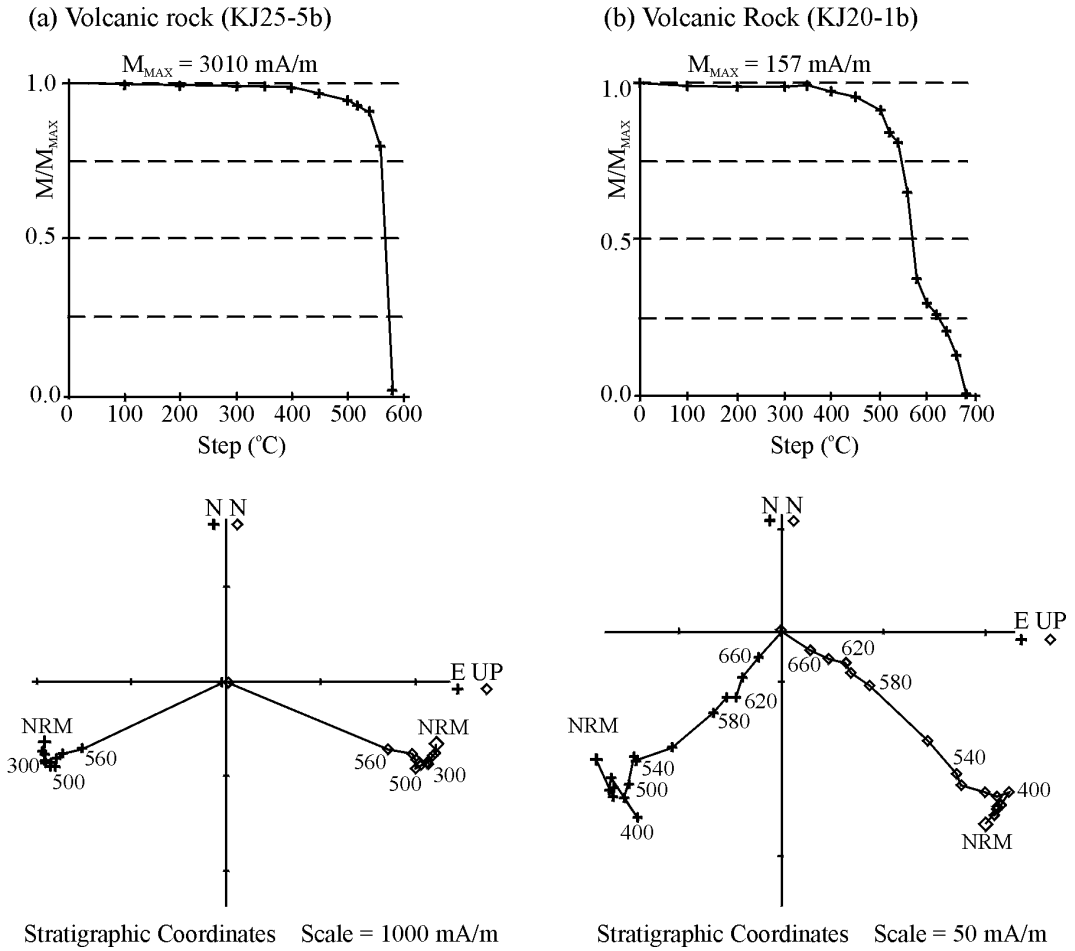


**Figure 5.** Typical thermal demagnetisation results of the volcanic rocks with normalized intensity curves and Zijderveld diagrams are shown.

during the stepwise unfolding test, even though the mean direction in stratigraphic coordinates seems statistically better when the *in situ* directions and 100 per cent tilt corrected directions are simply compared. Likewise the mean direction of ChRMs of the Gongju Group turns out to be $D/I = 23.9^\circ/50.6^\circ$ ($k = 95.5$, $\alpha_{95} = 3.9^\circ$) at 30 per cent unfolding with a maximum $k$ value. Generally, the results showing a maximum $k$ value at $30 \sim 70$ per cent unfolding are regarded as syntilting acquisition of magnetisation, the acquisition of remanence during a tectonic activity that caused the tilting of the strata. Incomplete isolation of the characteristic component is also a

**Table 2.** Palaeomagnetic results of the volcanic rocks in the Gongju Basin.

| Lithology | Site | n | Site | | Dg (°) | Ig (°) | Ds (°) | Is (°) | $k$ | $\alpha_{95}$ (°) | VGP | | $dp$ (°) | $dm$ (°) |
|---|---|---|---|---|---|---|---|---|---|---|---|---|---|---|
| | | | Long. (°E) | Lat. (°N) | | | | | | | Long. (°E) | Lat. (°N) | | |
| Volcanic | KJ17 | 19 | 127.10 | 36.47 | 243.0 | 87.1 | 19.7 | 39.9 | 58.1 | 5.6 | 250.6 | 68.1 | 4.0 | 6.7 |
| Rocks | KJ18 | 13 | 127.10 | 36.47 | 37.2 | −56.6 | 195.2 | −47.7 | 60.5 | 5.8 | 243.8 | 75.1 | 4.9 | 7.6 |
| | KJ19 | 12 | 127.10 | 36.47 | 3.1 | −33.9 | 207.3 | −46.3 | 101.5 | 4.0 | 230.3 | 65.3 | 3.3 | 5.1 |
| | KJ20 | 12 | 127.13 | 36.48 | 242.5 | −28.3 | 221.4 | −40.7 | 95.7 | 4.7 | 219.3 | 54.1 | 3.9 | 6.0 |
| | KJ21 | 12 | 127.13 | 36.48 | 245.1 | −26.6 | 218.5 | −37.8 | 154.9 | 3.2 | 230.9 | 53.3 | 2.2 | 3.8 |
| | KJ22 | 7 | 127.13 | 36.48 | 216.1 | −35.2 | 195.2 | −30.7 | 77.8 | 5.1 | 269.0 | 65.9 | 3.2 | 5.7 |
| | KJ23* | 8 | 127.13 | 36.48 | 84.3 | 72.6 | 132.6 | 39.7 | 2.0 | 55.5 | 172.1 | −15.9 | 40.0 | 66.6 |
| | KJ24* | 10 | 127.13 | 36.48 | 343.4 | 64.8 | 140.5 | 72.5 | 14.9 | 23.0 | 147.3 | 9.9 | 18.7 | 29.3 |
| | KJ25 | 11 | 127.13 | 36.48 | 284.4 | −6.7 | 218.0 | −52.6 | 152.7 | 3.7 | 211.8 | 58.8 | 3.5 | 5.1 |
| | KJ26 | 7 | 127.13 | 36.48 | 268.6 | −39.7 | 185.1 | −32.2 | 229.6 | 5.8 | 292.4 | 70.5 | 3.7 | 6.5 |
| | KJ27 | 9 | 127.13 | 36.48 | 293.1 | −18.4 | 200.7 | −60.6 | 52.6 | 7.7 | 193.1 | 73.2 | 8.9 | 11.7 |
| | Mean | 9/11 | | | 276.0 | −47.9 | | | 3.0 | 35.6 | | | | $K = 34.6$ |
| | | | | | | | 204.2 | −43.8 | 36.6 | 8.6 | 235.3 | 67.2 | | $A_{95} = 8.9$ |

n: number of samples; Dg and Ig: declination and inclination in geographic coordinates; Ds and Is: declination and inclination in stratigraphic coordinates; $k$: Fisherian precision parameter; $\alpha_{95}$: radius of cone of 95 per cent confidence interval; VGP: virtual geomagnetic pole; $dp$: the semi axis of the confidence ellipse along the great-circle path from site to pole; $dm$: the semi axis of the confidence ellipse perpendicular to that great-circle path; $K$: the best-estimate of the precision parameter $k$ for the observed distribution of site-mean VGPs; $A_{95}$: the radius of the 95 per cent confidence circle about the calculated mean pole.*: KJ23 and KJ24 are excluded from the calculation of formation mean direction.

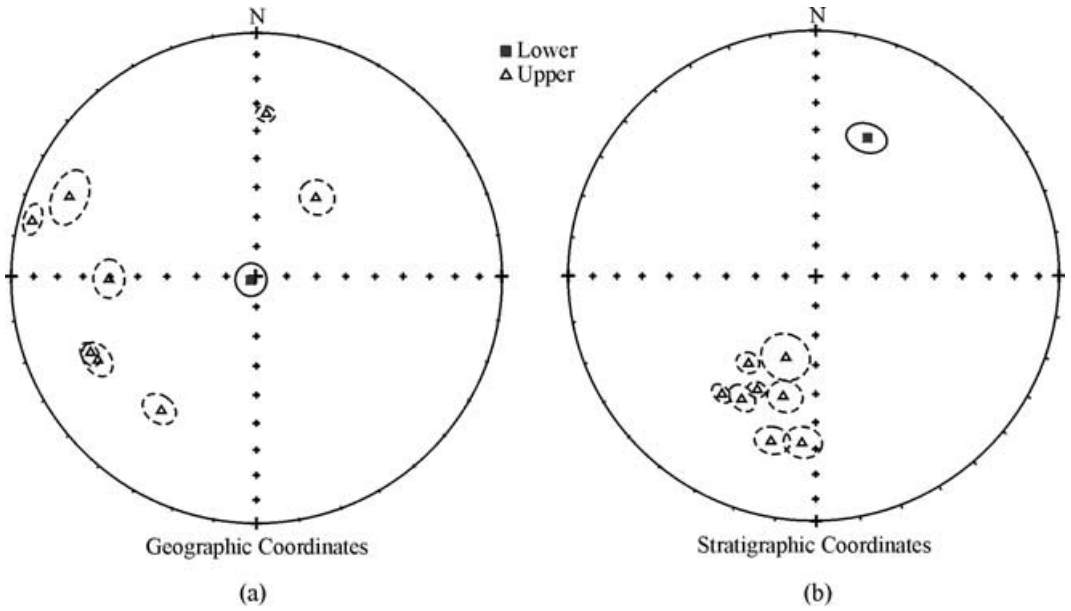


**Figure 6.** Equal area projections of the site mean directions with 95 per cent confidence circle of the volcanic rocks (a) in geographic and (b) stratigraphic coordinates.

common cause of the maximum $k$ being not at 0 per cent or 100 per cent untilting. However, this possibility can be ruled out, because the demagnetisation results indicate successful isolation of ChRMs. In addition, a tilt correction of strata with an initial dip of about 10° or less may erroneously yield a result of the syntilting acquisition of magnetisation. When the Gongju Group, whose mean dip angle is about 45°, is 30 per cent untilted, the dip angle becomes about 32.5°. This angle is steep enough to be distinguished from the effect of the initial slope of the sedimentary strata. Thus, it is believed that the characteristic component of the Gongju Group is remagnetised at the time of tilting of the strata after the formation of the Group.

The pole position of the Gongju Group for the 30 per cent untilted direction (Lat./Long. = 69.6°N/224.3°E, $dp = 3.5°$, $dm = 5.2°$) is statistically different from those of the middle Early and late Early Cretaceous, Tertiary and Quaternary periods. Instead it is located between the late Early Cretaceous and Tertiary periods on a presumable segment of the apparent polar wander path (APWP) of Korea (Fig. 11a). On the other hand, the palaeomagnetic results and electron microscope observations of the volcanic rocks indicate that the ChRM of the volcanic rocks is the primary remanence carried by magnetite and/or haematite of igneous origin. When the palaeomagnetic pole position of the volcanic rocks (Lat./Long. = 67.2°N/235.3°E, $A_{95} = 8.9°$) is compared with that of the Gongju

**Table 3.** The K–Ar ages of the volcanic rock samples occurring as a dyke rocks (K-1) and volcanic flows (K-2, K-3 and K-4) covering sedimentary layer in the study area.

| Sample | *K* (wt%) | *K* (wtg) | $^{36}Ar^*$ ($10^{-10}$ cm$^3$ g$^{-1}$) | $^{40}Ar^*$ ($10^{-8}$ cm$^3$ g$^{-1}$) | Age (Ma) |
|---|---|---|---|---|---|
| K-1 | 1.314 | 0.01421 | 12.493 | 427.102 | 81.84 ± 2.40 |
| K-2 | 4.061 | 0.01268 | 17.239 | 1182.858 | 73.51 ± 2.16 |
| K-3 | 4.005 | 0.01302 | 11.627 | 1276.916 | 80.32 ± 2.36 |
| K-4 | 1.017 | 0.01657 | 14.021 | 309.608 | 76.77 ± 2.26 |

*: $^{36}Ar$ and $^{40}Ar$ are given in STP (standard temperature pressure) system.

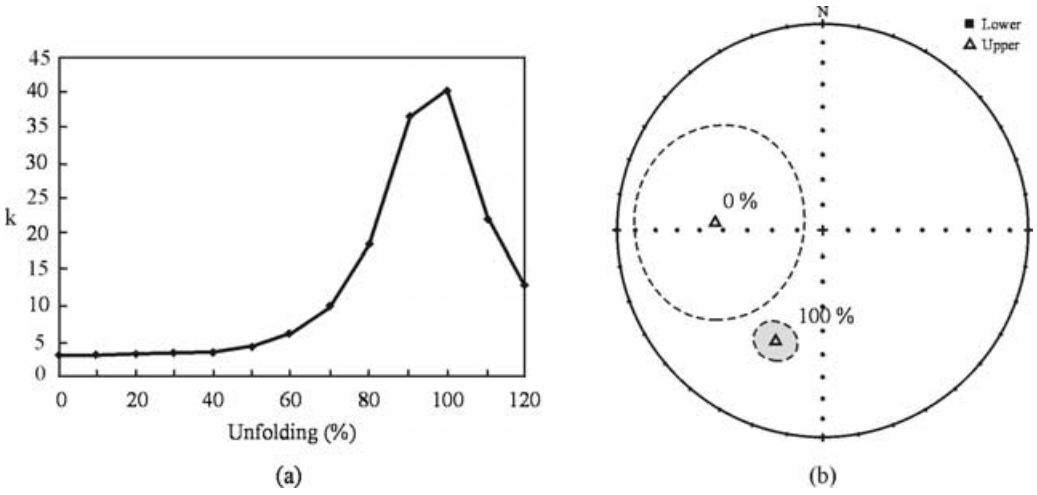


**Figure 7.** Results of the stepwise unfolding test of the volcanic rocks. (a) Plot of Fisher's precision parameter (*k*) versus per cent unfolding and (b) palaeomagnetic directions at 0 per cent and 100 per cent unfolding are shown.

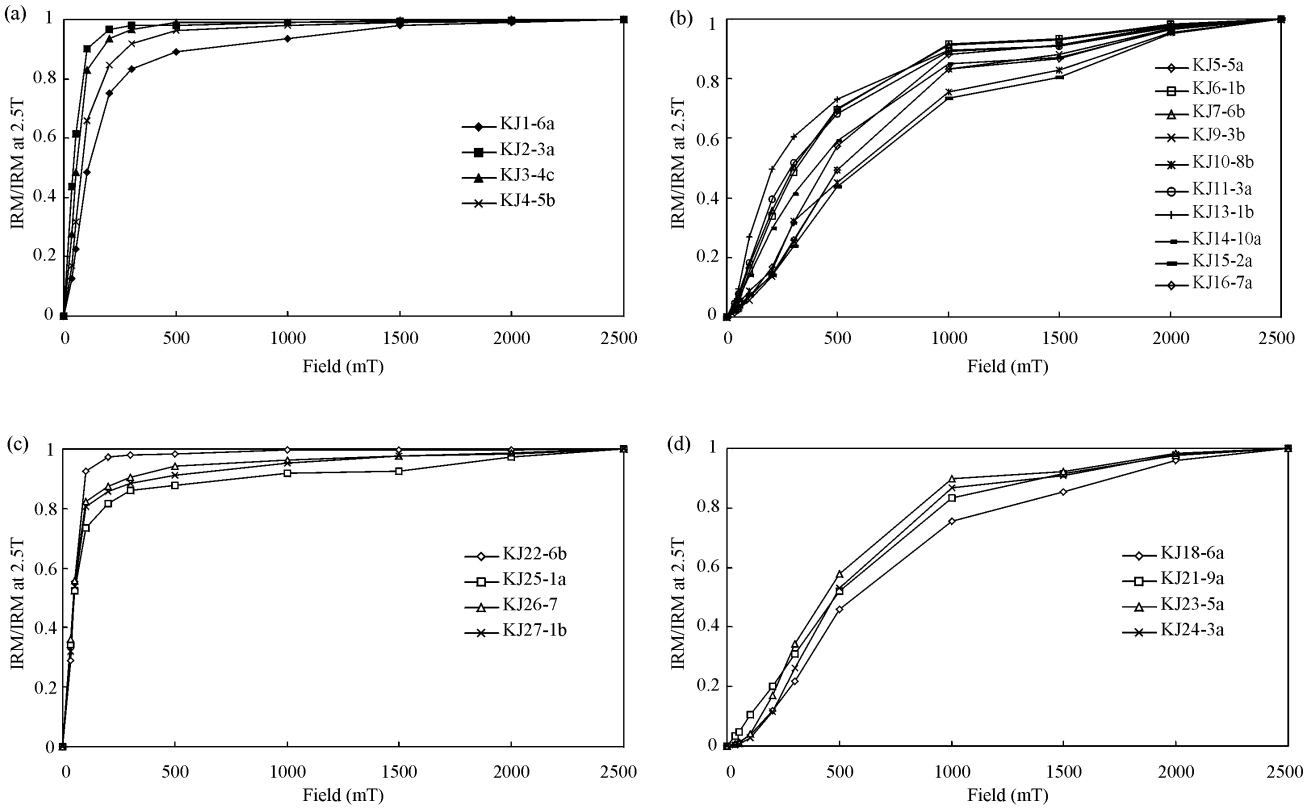


**Figure 8.** IRM acquisition curves for (a) the Hwayangri Formation, (b) the Sinheungri Formation, and (c) the magnetite-dominant and (d) haematite-dominant patterns of the volcanic rocks.

**Table 4.** Hysteresis properties of representative samples.

| Sample | $H_{cr}$ (mT) | $H_c$ (mT) | $H_{cr}/H_c$ | $M_{rs}$ ($\mu$Am$^2$) | $M_s$ ($\mu$Am$^2$) | $M_{rs}/M_s$ | Formation | Rock type |
|---|---|---|---|---|---|---|---|---|
| KJ1-4 | 78.19 | 9.00 | 8.69 | 0.70 | 66.88 | 0.01 | Hwayangri | Black shale |
| KJ2-3b | 60.98 | 32.50 | 1.88 | 14.08 | 115.96 | 0.12 | | Black shale |
| KJ3-4b | 47.49 | 8.00 | 5.94 | 0.98 | 87.53 | 0.01 | | Black shale |
| KJ4-2b | 68.51 | 24.00 | 2.85 | 5.21 | 92.49 | 0.06 | | Black shale |
| KJ5-5b | 265.42 | 72.00 | 3.69 | 1.93 | 19.65 | 0.10 | Sinheungri | Red shale |
| KJ6-9a | 134.79 | 38.50 | 3.50 | 2.39 | 36.34 | 0.07 | | Red shale |
| KJ7-6b | 314.15 | 21.00 | 14.96 | 3.61 | 73.61 | 0.05 | | Red shale |
| KJ8-1c | 52.34 | 16.00 | 3.27 | 1.38 | 21.18 | 0.07 | | Gray sandstone |
| KJ9-1b | 532.07 | 54.00 | 9.85 | 1.88 | 28.58 | 0.07 | | Red siltstone |
| KJ10-5b | 572.82 | 58.00 | 9.88 | 2.64 | 32.61 | 0.08 | | Red siltstone |
| KJ11-4b | 143.20 | 36.50 | 3.92 | 3.30 | 45.74 | 0.07 | | Red siltstone |
| KJ12-4b | 147.29 | 36.00 | 4.09 | 4.93 | 64.63 | 0.08 | | Red shale |
| KJ13-10b | 97.08 | 31.00 | 3.13 | 3.97 | 62.35 | 0.06 | | Red siltstone |
| KJ14-2b | 413.21 | 35.50 | 11.64 | 3.05 | 58.60 | 0.05 | | Red siltstone |
| KJ15-9b | 588.10 | 35.00 | 16.80 | 3.21 | 67.51 | 0.05 | | Red siltstone |
| KJ16-4 | 524.50 | 40.00 | 13.11 | 2.74 | 50.64 | 0.05 | | Red siltstone |
| KJ17-6b | 239.39 | 161.00 | 1.49 | 11.34 | 37.80 | 0.30 | Volcanic rocks | |
| KJ18-4b | 676.63 | 41.00 | 16.50 | 3.20 | 67.80 | 0.05 | | |
| KJ19-4B | 34.00 | 10.00 | 3.40 | 23.09 | 277.13 | 0.08 | | |
| KJ20-7b | 173.81 | 43.50 | 4.00 | 4.55 | 78.03 | 0.06 | | |
| KJ21-2 | 182.49 | 116.00 | 1.57 | 12.62 | 29.33 | 0.43 | | |
| KJ22-7b | 96.87 | 44.00 | 2.20 | 6.64 | 54.56 | 0.12 | | |
| KJ23-5b | 434.51 | 44.00 | 9.88 | 1.69 | 35.34 | 0.05 | | |
| KJ24-6 | 496.72 | 39.50 | 12.58 | 1.29 | 29.80 | 0.04 | | |
| KJ25-7b | 28.80 | 226.00 | 0.13 | 103.71 | 301.07 | 0.34 | | |
| KJ26-8a | 42.45 | 24.00 | 1.77 | 5.08 | 104.10 | 0.05 | | |
| KJ27-6b | 108.77 | 58.00 | 1.88 | 13.95 | 94.78 | 0.15 | | |

$H_{cr}$: coercivity of remanence, $H_c$: coercive force, $M_{rs}$: saturation remanence, $M_s$: saturation magnetisation.

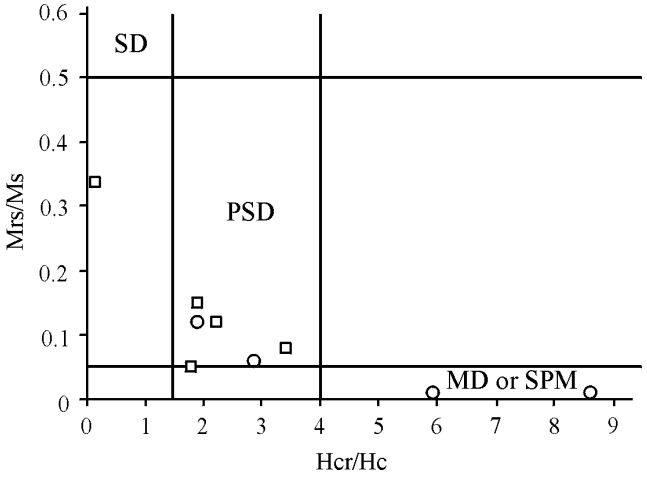


**Figure 9.** Hysteresis properties and domain state of samples from the Hwayangri (open circles) and the volcanic rocks (open squares) (after Day *et al.* 1977).

Group, it is evident that the palaeomagnetic pole of the volcanic rocks is statistically same as that of the 30 per cent untilted direction of the Gongju Group, because the two poles are plotted inside the 95 per cent cones of confidence of each other (Fig. 11a). On the basis of the comparison of palaeomagnetic pole positions, it is interpreted that the volcanic rocks acquired the primary ChRMs almost at the same time as the remagnetisation of the Gongju Group. In addition, the K–Ar ages of the volcanic rocks ranging from $81.8 \pm 2.4$ Ma to $73.5 \pm 2.2$ Ma indicate Campanian stage of the Late Cretaceous. Thus, it is believed that the acquisition of the primary magnetisation of the volcanic rocks and the remagnetisation of the Gongju Group had been accomplished during the Late Cretaceous.

### 7.2 The mechanism of remagnetisation

There are two different explanations for the remagnetisation processes. One is the realignment of magnetisation within the pre-existing magnetic minerals to the ambient field when those are exposed to the elevated temperature above $250 \sim 300^{\circ}$C and below the Curie temperature of the magnetic minerals for a prolonged period of time. This will affect the ability of the magnetic minerals to retain a primary NRM and cause acquisition of thermoviscous remanent magnetisation (TVRM) (Kent 1985; Jackson 1990) based on the theoretical blocking temperature-relaxation time curves of Pullaiah *et al.* (1975). The other process involves a chemical remanent magnetisation (CRM) acquired when new magnetic minerals formed long after the formation of the rocks at low temperature. The formation of new magnetic minerals is commonly accompanied by migration of orogenic or basinal fluids, or possibly migration of hydrocarbons (McCabe *et al.* 1983; Oliver 1986; Elmore & McCabe 1991). In addition, surface weathering is reportedly a possible cause of the remagnetisation of rocks (Otofuji *et al.* 1989). The palaeomagnetic directions from the Gongju Group, however, are very well clustered with a uniform polarity. Moreover, iron-oxides, as magnetic carriers in the Sinheungri Formation, found by electron microscope observations are not the products of weathering process. Therefore, the weathering process is not responsible for the remagnetisation.

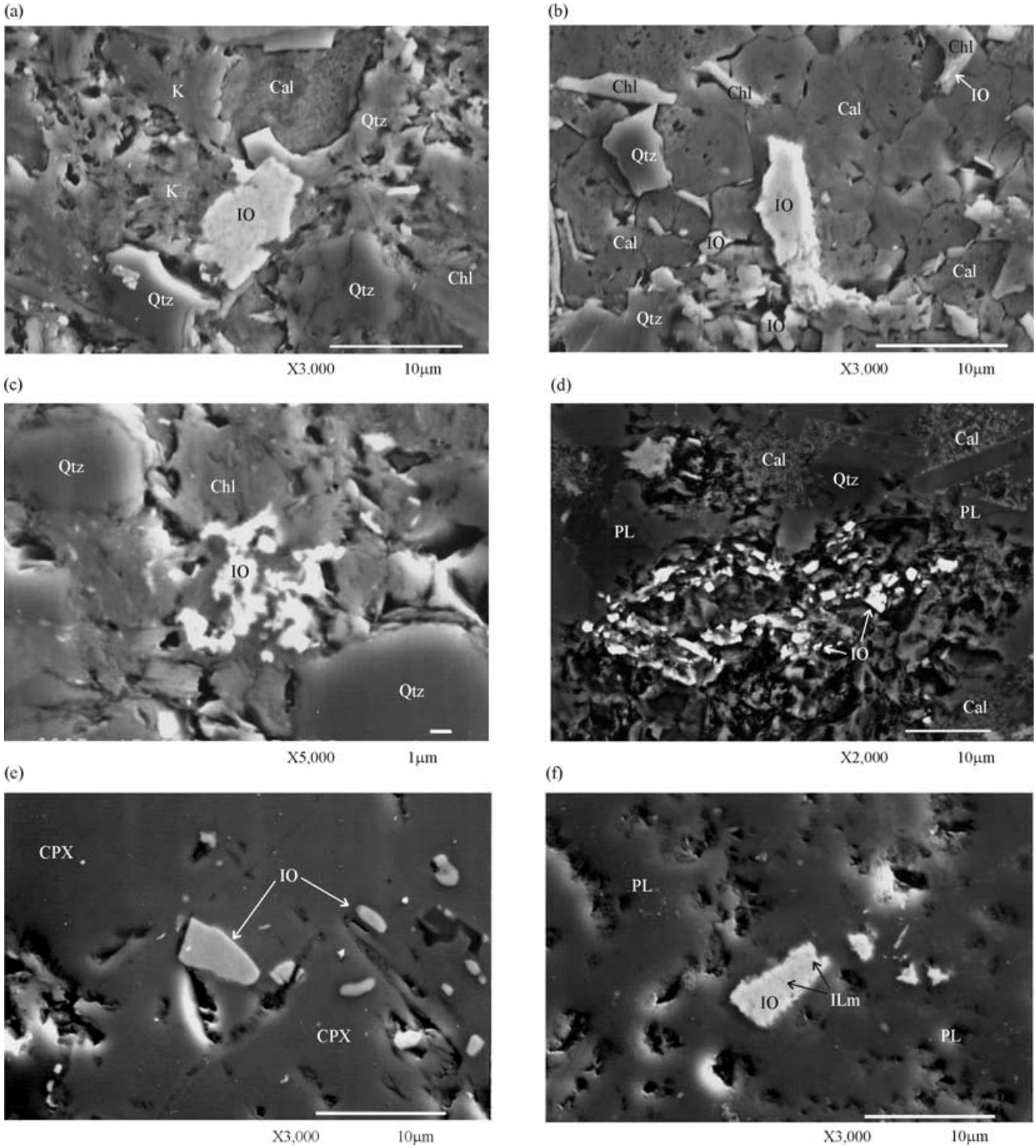


**Figure 10.** Secondary electron image (SEI) of magnetic minerals in samples of the Sinheungri Formation and the volcanic rocks. (a) Large iron-oxide grains authigenically filled in a void surrounded by quartz, K-feldspar and calcite. (b) A large void-filling iron-oxide in the centre and submicron size needle shaped iron-oxide grains within the cleavage of chlorite in the upper-right corner are shown. (c) Aggregates of iron-oxide grains around chlorite grain boundaries. (d) Small iron-oxide grains of submicron to 2 $\mu$m in length precipitated in the pore spaces. (e) Anhedral to subhedral iron-oxide grains of about 0.1 $\sim$ 7 $\mu$m in length are shown. (f) Iron-oxide grains with ilmenite lamella in plagioclase grains are observed. IO: iron-oxide; *K*: K-feldspar; Cal: calcite; Chl: chlorite; Qtz: quartz; PL: plagioclase; CPX: clinopyroxene; Ilm: ilmenite.

TVRM is most likely to have occurred in rocks when they were buried to depths on the order of kilometres for millions of years (Kent 1985) or under the influence of igneous activities. For instance, in order to acquire TVRM lower than the unblocking temperature of 640 $\sim$ 660°C for haematite, it is needed to be heated above 550°C for at least 10 million years based on the blocking temperature-relaxation time curves of Pullaiah *et al.* (1975). Such high temperature condition should have resulted in considerable degree of

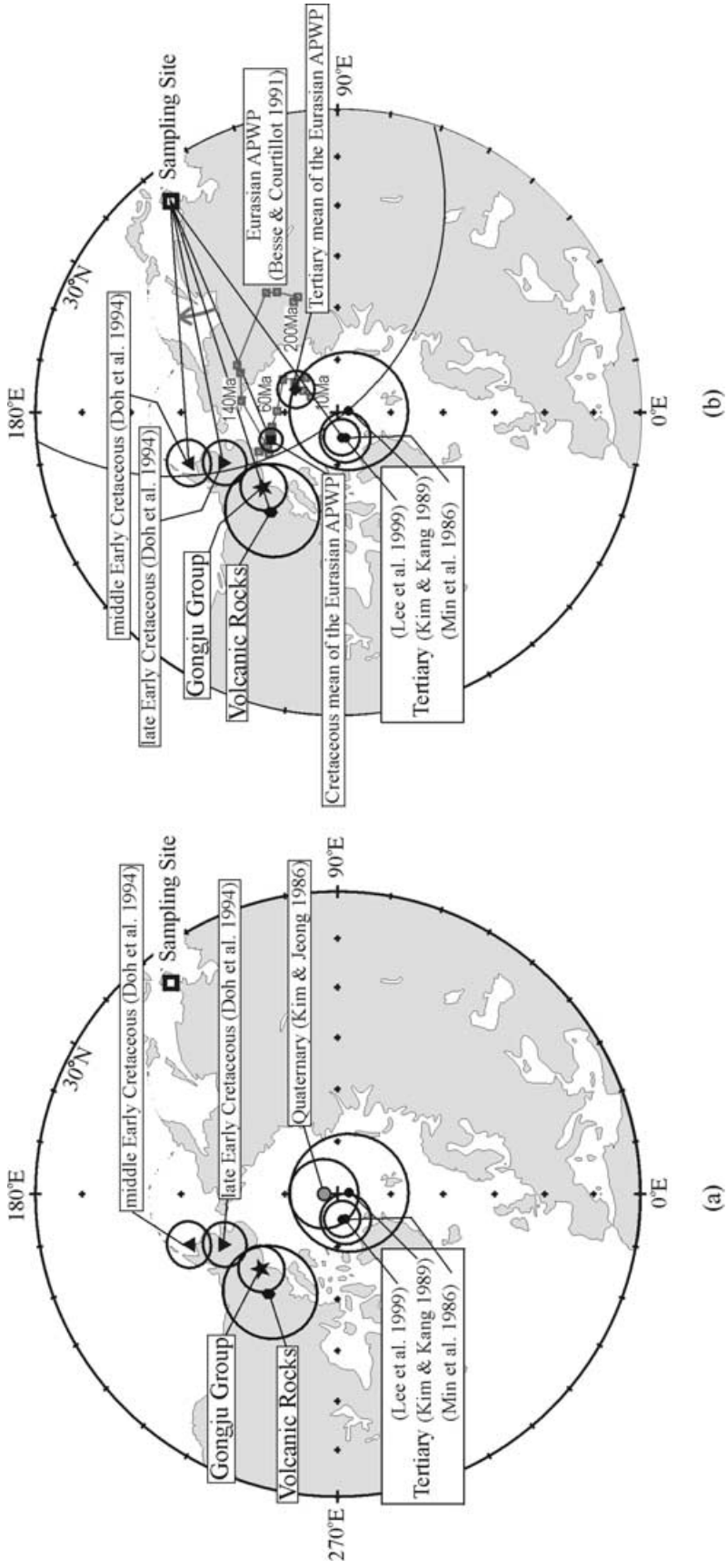


**Figure 11.** Palaeomagnetic poles of the Gongju Group calculated from the 30 per cent untilted site mean direction and of the volcanic rocks in the Gongju Basin compared with (a) those of middle Early Cretaceous to Quaternary Periods in Korea, and (b) those of Cretaceous in Eurasia.

**Table 5.** Cretaceous palaeomagnetic poles and recalculated directions for Korea and Eurasia.

| Period | Palaeomagnetic poles | | Palaeomagnetic directions | | Rotations $R \pm \Delta R$ (Korea with respect to Eurasia) |
|---|---|---|---|---|---|
| | Korea | Eurasia | Korea | Eurasia | |
| Late Cretaceous | 235.3°E, 67.2°N ($A_{95} = 8.9°$) (This study) | | $D/I = 24.2°/43.8°$ ($\alpha_{95} = 8.6°$) | | $7.1° \pm 9.8°$ |
| late Early Cretaceous | 204.1°E, 66.4°N ($A_{95} = 4.2°$) (Doh *et al.* 1994) | 202.8°E, 76.3°N ($A_{95} = 2.2°$) (Mean of 65–130 Ma, Besse & Courtillot 1991) | $D/I = 29.7°/57.5°$ ($\alpha_{95} = 3.3°$) | $D/I = 17.1°/58.0°$ ($\alpha_{95} = 1.9°$) | $12.6° \pm 5.4°$ |
| middle Early Cretaceous | 198.8°E, 59.9°N ($A_{95} = 4.3°$) (Doh *et al.* 1994) | | $D/I = 38.3°/59.1°$ ($\alpha_{95} = 3.1°$) | | $21.2° \pm 5.3°$ |

$A_{95}$: radius of 95 per cent confidence circle of the pole; $\alpha_{95}$: radius of cone of 95 per cent confidence interval; D/I: declination/inclination recalculated at the sampling site (127.13°E, 36.48°N). $R$: azimuthal rotation clockwise (+) or counter-clockwise (−); $\Delta R$: uncertainty (95 per cent limits) of $R$, estimated by the method of Demarest (1983).

metamorphism in rocks. However, neither are any intrusives found in and around the study area, nor do the samples in the study area show any signs of high temperature metamorphism, suggesting that TVRM as the mechanism for the remagnetisation in the study area can be discarded.

The electron microscope observations of samples from the Sinheungri Formation (Fig. 10) suggest that the magnetic minerals in the rocks are secondary (authigenic) in origin. Thus, it is interpreted that the major process that caused the remagnetisation in the rocks of the study area was chemical in nature. The CRM was acquired when the authigenic magnetic minerals formed long after the deposition of the Gongju Group under the influence of fluids. A previously reported K–Ar age from a hydrothermal vein in an adjacent area (71 Ma for sericite in the Seogseong mine, Shin & Jin 1995) supports that the fluid-mediated process would have been activated in the study area during the Late Cretaceous. The Kula/Pacific plates had subducted under the Eurasian plate during the Cretaceous (Sillitoe 1977). The oblique compressive force due to the Andean-type subduction caused the basement shoal in the southwestern Korean Peninsula and the sinistral movement in the fault systems (Chun & Chough 1992). This tectonic event probably played a major role for the volcanism in the northeastern part of the Gongju Basin, and for the migration of orogenic fluids through the fault system, which caused the remagnetisation of the Gongju Group. It is even possible to speculate that the formation of the volcanic rocks in the Gongju Basin might cause the fluid-mediated remagnetisation of the Gongju Group during the Late Cretaceous. Similar aspects of remagnetisation are observed in the Eumseong Basin (Doh *et al.* 1999) and the Yeongdong Basin (Doh *et al.* 1996) in the northern and southern boundaries of the Ogcheon Belt, respectively (Fig. 1).

### 7.3 The Cretaceous clockwise rotation of the Korean Peninsula

The Cretaceous palaeomagnetic poles of Korea are compared with the APWP of Eurasia (Besse & Courtillot 1991) to verify the relative tectonic evolution of the Korean Peninsula (Fig. 11b). The Korean Cretaceous poles obtained from the Gongju and Gyeongsang basins and the coeval Eurasian pole are plotted along a small circle centred at the reference point (the study area), showing that the Korean Cretaceous poles are displaced eastwards with respect to the Eurasian pole. This implies that the Korean Peninsula was located at the similar palaeolatitude to that of Eurasia and underwent clockwise rotations during the Cretaceous Period. In order to determine the magnitude of rotations of the Korean Peninsula, declinational differences are estimated between the palaeomagnetic directions of the Cretaceous rocks of the Korean Peninsula and the mean direction of Eurasia, which is recalculated for the sampling site of the present study from palaeomagnetic poles of 130 ∼ 65 Ma time interval (Table 5). The declinational differences indicate that the Korean Peninsula rotated $21.2° \pm 5.3°$, $12.6° \pm 5.4°$ and $7.1° \pm 9.8°$ clockwise with respect to Eurasia for the middle Early, late Early and Late Cretaceous, respectively.

The rotation mechanisms explained by recent palaeomagnetic studies revealing the Cretaceous clockwise rotation of the Korean Peninsula with respect to the adjacent major blocks are classified into two categories. One involves that the sinistral motion of the Tan-Lu Fault (Fig. 12) caused the clockwise rotation of the Korean Peninsula (Ma *et al.* 1993; Doh & Piper 1994; Uno & Chang 2000), and the other attributes the rotation to the Kula-Eurasia convergence (Zhao *et al.* 1999). The oblique subduction of the Kula plate initiated a sinistral movement along the NE–SW trending fault systems (Chun & Chough 1992), and might cause local anti-clockwise rotations of some microblocks, which can be illustrated by the ball bearing model (Well & Coe 1985), bounded by major faults such as the Gongju and Gwangju faults (Kim & Noh 1993; Kim *et al.* 1997; Lim *et al.* 2001) (Fig. 1). The Kula-Eurasia convergence by itself, however, cannot explain the clockwise rotation of the Korean Peninsula because the clockwise rotations were observed not only in the fault bounded blocks, such as the Ogcheon Belt (Doh & Piper 1994), but also in the Gyeongsang Basin (Zhao *et al.* 1999) and the Gyeonggi Massif (this study; Uno & Chang 2000), outside the faults (Fig. 12). On the other hand, it was reported that the maximum horizontal displacement due to the sinistral movement of the Tan-Lu Fault, necessary for the clockwise rotation of the Korean Peninsula, since the Late Triassic was more than 700 km (Xu 1980) and the sinistral motion had been active until the Late Cretaceous (Klimetz 1983). In addition, a previous palaeomagnetic study (Uchimura *et al.* 1996) from the Benxi area, east to the Tan-Lu Fault, showed that the clockwise rotation ($17.9° \pm 9.8°$) related to the sinistral motion of the Tan-Lu Fault by comparing the Cretaceous poles from two sides of the fault indeed occurred during the post-Cretaceous time. It can be speculated that the Korean Peninsula, southeastern part of the Tan-Lu Fault, had been tectonically affected by the sinistral

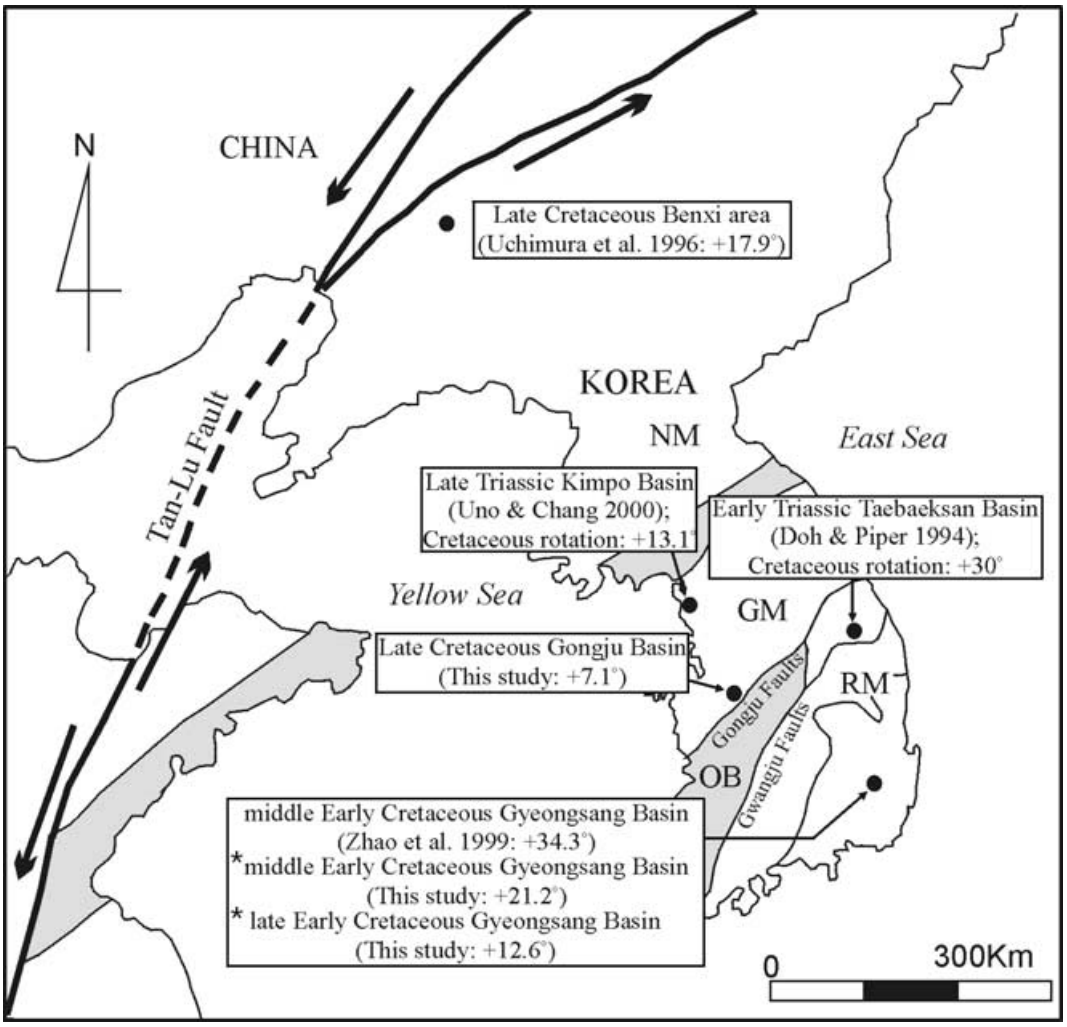


**Figure 12.** Schematic map of the Far East Asia, showing magnitudes of clockwise rotation of the Korean Peninsula with respect to the adjacent major block during the Cretaceous (*: recalculated data of Doh *et al.* 1994). Symbols are same as in Fig. 1.

motion of the fault in a similar way to the Benxi area had, thus it is tentatively interpreted that the sinistral motion of the Tan-Lu Fault played an important role in the clockwise rotation of the peninsula. Although Uchimura *et al.* (1996) assigned the timing of the rotation as the post-Cretaceous period based on the mean pole of the Early and Late Cretaceous rocks, it can be argued that the rotation might occur after the formation of the sedimentary rocks, even during the Cretaceous Period, because their age constraints of the investigated rocks and the pole were poorly defined. On the contrary, the palaeomagnetic results of this study, firmly supported by the K–Ar age determinations, show that the clockwise rotations of the Korean Peninsula occurred during the Cretaceous Period and that the rotations might have ceased after the Cretaceous Period based on the fact that the declinational difference between the Tertiary palaeomagnetic poles from the peninsula and the coeval Eurasian pole is not large enough to deduce the relative rotation of the two blocks (Fig. 11b).

## 8 CONCLUSIONS

It is found that the Gongju Group was remagnetised during the tilting of strata yielding the ChRM direction of $D/I = 23.9^\circ/50.6^\circ$ ($k = 95.5$, $\alpha_{95} = 3.9^\circ$) at 30 per cent untilting of the strata with a maximum value of precision parameter ($k$), while the volcanic rocks, whose K–Ar ages range from 81.8 ± 2.4 Ma to 73.5 ± 2.2 Ma, are revealed to acquire primary remanence with the direction of $D/I = 204.2^\circ/-43.8^\circ$ ($k = 36.6$, $\alpha_{95} = 8.6^\circ$) in stratigraphic coordinates. The palaeomagnetic pole positions are at Lat./Long. = 69.6°N/224.3°E ($dp = 3.5^\circ$, $dm = 5.2^\circ$) calculated for the 30 per cent tilt-corrected direction of the Gongju Group and at Lat./Long. = 67.2°N/235.3°E ($A_{95} = 8.9^\circ$) for the volcanic rocks. The volcanic rocks acquired their primary magnetisation almost at the same time as the chemical remagnetisation of the Gongju Group in Campanian stage of the Late Cretaceous. Because of the sinistral motion of the Tan-Lu Fault, the Korean Peninsula rotated 21.2° ± 5.3°, 12.6° ± 5.4°, and 7.1° ± 9.8° clockwise with respect to Eurasia for the middle Early, late Early and Late Cretaceous, respectively.

## ACKNOWLEDGMENTS

This study was supported by the BK21 project (Division of Earth and Environmental Sciences, Korea University). We deeply appreciate the constructive comments of Dr R. Van der Voo and an

anonymous reviewer. Editorial guidance was provided by Prof. Cor G. Langereis.

## REFERENCES


Besse, J. & Courtillot, V., 1991. Revised and synthetic polar wander paths of the African, Eurasian, North American and Indian plates, and true polar wander since 200 Ma, *J. geophys. Res.,* **96,** 4029–4050.

Choi, H.I., 1999. Upper Mesozoic Strata, in *Geology of Korea,* eds, Lee, J.H., Won, C.K., Kim, J.H. & Lee C.Z., pp. 233–267, *Geol. Soc., Korea,* Sigma Press, Seoul.

Chun, S.S. & Chough, S.K., 1992. Tectonic history of Cretaceous sedimentary basins in the southwestern Korean Peninsula and Yellow Sea, in *Sedimentary Basins in the Korean Peninsula and Adjacent Seas,* pp. 60–76, ed. Chough, S.K., Hanlim Pub., Seoul.

Day, R., Fuller, M. & Schmidt, V.A., 1977. Hysteresis properties of titanomagnetite: grain-size and compositional dependence, *Phys. Earth planet. Inter.,* **13,** 260–267.

Demarest, H.H., 1983. Error analysis of the determination of tectonic rotation from palaeomagnetic data, *J. geophys. Res.,* **88,** 4321–4328.

Doh, S.J. & Kim, K.H., 1994. A palaeomagnetic study of Cretaceous rocks from the Euiseong area, *Econ. Environ. Geol.,* **27,** 263–279.

Doh, S.J. & Piper, J.D.A., 1994. Palaeomagnetism of the (Upper Palaeozoic-Lower Mesozoic) Pyeongan Supergroup, Korea: a Phanerozoic link with the North China Block, *Geophys. J. Int.,* **117,** 850–863.

Doh, S.J., Hwang, C.S. & Kim, K.H., 1994. A palaeomagnetic study of sedimentary rocks from Gyeongsang Supergroup in Milyang Sub-basin, *J. geol. Soc. Korea,* **30,** 211–228.

Doh, S.J., Cho, Y.Y. & Suk, D.W., 1996. Remagnetisation of the Cretaceous sedimentary rocks in the Yeongdong Basin, *Econ. Envron. Geol.,* **29,** 193–206.

Doh, S.J., Suk, D.W. & Kim, B.Y., 1999. Palaeomagnetic and rock-magnetic studies of Cretaceous rocks in the Eumseong Basin, Korea, *Earth Planets Space,* **51,** 337–349.

Elmore, R.D. & McCabe, C., 1991. The occurrence and origin of remagnetisation in the sedimentary rocks of North America, *Rev. Geophys.,* suppl. (IUGG Report), **29,** 377–383.

Gradstein, F.M., Agterberg, F.P., Ogg, J.G., Hardenbol, J., van Veen, P., Thierry, J. & Huang, Z., 1994. A Mesozoic time scale, *J. geophys. Res.,* **99,** 24 051–24 074.

Jackson, M., 1990. Diagenetic sources of stable remanence in remagnetised Paleozoic cratonic carbonates: A rock magnetic study, *J. geophys. Res.,* **95,** 2753–2761.

Kent, D.V., 1985. Thermoviscous remagnetisation in some Appalachian limestones, *Geophys. Res. Lett.,* **12,** 805–808.

Kim, K.H. & Jeong, B.I., 1986. A study on the palaeomagnetism of southern Korea since Permian, *J. Korean Inst. Mining Geol.,* **19,** 67–83.

Kim, I.S. & Kang, H.C., 1989. Palaeomagnetism of Tertiary rocks in the Eoil Basin and its vicinities, southeast Korea, *J. geol. Soc. Korea,* **25,** 273–293.

Kim, K.H. & Kim, D.S., 1991. Magnetostratigraphy of the Chaeyaksan, Konchonri, and Jusasan formations distributed in Taeku-Kyongju area, *J. geol. Soc. Korea,* **27,** 40–51.

Kim, K.H. & Noh, B.S., 1993. Palaeomagnetic Study of the Cretaceous Rocks in the Ogcheon Belt: Palaeomagnetism of the Sedimentary Rocks in the Neungju Basin, *J. Kor. Earth Sci. Soc.,* **14,** 44–57.

Kim, K.H., Song, M.Y., Jeong, J.G., Kim, W.S. & Lee, D.W., 1997. Structure and Physical Properties of the Mid-west Crust of Korea (III): Palaeomagnetism of the Cretaceous Volcanic Rocks in the Southern Choogaryong Rift Zone, *J. Kor. Earth Sci. Soc.,* **18,** 332–338.

Kirschvink, J.L., 1980. The least square line and plane and the analysis of palaeomagnetic data, *Geophys. J. R. astr. Soc.,* **62,** 699–718.

Klimetz, M.P., 1983. Speculations on the Mesozoic plate tectonic evolution of Eastern China, *Tectonics,* **2,** 139–166.

Lee, D.S., ed., 1988. *Geology of Korea,* Kyohak-Sa Publishing Co., Seoul.

Lee, J.Y., 1990. Structural Evolution of the Gongju Basin, *PhD thesis,* Seoul National University, Seoul.

Lee, Y.S., Ishikawa, N. & Kim, W.K., 1999. Palaeomagnetism of Tertiary rocks on the Korean Peninsula: tectonic implications for the opening of the East Sea (Sea of Japan), *Tectonophysics,* **304,** 131–149.

Lee, G.D., Besse, J. & Courtillot, V., 1987. Eastern Asia in the Cretaceous: New palaeomagnetic data from south Korea and a new look at Chinese and Japanese data, *J. geophys. Res.,* **92,** 3580–3596.

Lee, M.W, Won, C.K. & Kim, K.H., 1992. The Cretaceous volcanic activities and petrology in Gyeonggi Massif—On the Gapcheon, Eumseong and Gongju basins-, *J. geol. Soc. Korea,* **28,** 314–333.

Lim, M., Lee, Y.S., Kang, H.C., Kim, J.Y. & Park, I.H., 2001. Palaeomagnetic Study on Cretaceous Rocks in Haenam Area, *Econ. Environ. Geol.,* **34,** 119–131.

Ma, X., Yang, Z. & Xing, L., 1993. The Lower Cretaceous reference pole for North China, and its tectonic implications, *Geophys. J. Int.,* **115,** 323–331.

McCabe, C., Van der Voo, R., Peacor, C.R., Scotese, C.R. & Freeman, R., 1983. Diagenetic magnetite carries ancient secondary remanence in some Palaeozoic sedimentary carbonates, *Geology,* **11,** 221–223.

Min, K.D., Kim, O.J., Yun, S.K., Lee D.S. & Joo, S.H., 1982. Applicability of the plate tectonics to the post-Late Cretaceous igneous activity and mineralisation in the southern part of south Korea (I), *J. Korean Inst. Mining Geol.,* **15,** 123–154.

Min, K.D., Won, J.S. & Hwang, S.Y., 1986. Palaeomagnetic Study on the Volcanic and Sedimentary Rocks of Jeju Island, *J. Korean Inst. Mining Geol.,* **19,** 153–163.

Nagao, K., Ogata, A., Miura, Y.N. & Yamaguchi, K., 1996. Ar isotope analysis for K–Ar dating using two modified-VG5400 mass spectrometer-1: isotope dilution method, *J. Mass. Spectrom. Soc. Japan,* **44,** 39–61.

Oliver, J., 1986. Fluids expelled tectonically from orogenic belts: Their role in hydrocarbon migration and other geologic phenomena, *Geology,* **14,** 99–102.

Otofuji, Y., Oh, J.Y., Hirajima, T., Min, K.D. & Sasajima, S., 1983. Palaeomagnetism and age determination of Cretaceous rocks from Gyeongsang Basin, Korean peninsula, in *The Tectonic and Geologic Evolution of Southeast Asian Seas and Islands, Part 2, Geophys. Monogr. 27,* pp. 388–396, ed. Hays, D.E., Am. geophys. Un., Washington, DC.

Otofuji, Y., Kim, K.H., Inokuchi, H., Morinaga, H., Murata, F., Katao, H. & Yaskawa, K., 1986. A palaeomagnetic reconnaissance of Permian to Cretaceous sedimentary rocks in southern part of Korean Peninsula, *J. Geomag. Geoelectr.,* **38,** 387–402.

Otofuji, Y., Katsuargi, K., Inokuchi, H., Yaskawa, K., Kim, K.H., Lee, D.S. & Lee, H.Y., 1989. Remagnetisation of Cambrian to Triassic sedimentary rocks of the Paegunsan Syncline of the Ogcheon Zone, South Korea, *J. Geomag. Geoeletr.,* **41,** 119–135.

Pullaiah, G., Irving, E., Buchan, K.L. & Dunlop, D.J., 1975. Magnetisation changes caused by burial and uplift, *Earth planet. Sci. Lett.,* **28,** 133–143.

Shin, S.C. & Jin, M.S., 1995. Isotope age map of ore deposits in Korea (1:1,000,000), Korea Institute of Geology, Mining and Materials, Daejeon.

Sillitoe, R.H., 1977. Metallogeny of an Andean-type continental margin in south Korea: Implications for opening of the Japan Sea, in *Island Arcs, Deep Sea Trenches and Back-Arc basins, Maurie Ewing Ser. I,* pp. 303–310, eds Talwani, M. & Pitman, W.C., Am. Geophys. Un., Washington, DC.

Song, M.-Y., Lee, J.-Y., Lee, C.-Z. & Lee, D.-I., 1991. Integrated Geotectonic Study on the Mesozoic Sedimentary basins in Eumseong-Jeungpyeong and Gongju Area (II. Gongju Basin), *J. Kor. Earth Sci. Soc.,* **12,** 1–13.

Uchimura, H., Kono, M., Tsunakawa, H., Kimura, G., Wei, Q., Hao, T. & Liu, H., 1996. Palaeomagnetism of late Mesozoic rocks from northern China: the role of the Tan-Lu fault in the North China Block, *Tectonophysics,* **262,** 301–319.

Uno, K. & Chang, K.-H., 2000. Palaeomagnetic results from the lower Mesozoic Daedong Supergroup in the Gyeonggi Block, Korean Peninsula, *Earth planet. Sci. Lett.,* **182,** 49–59.

Van der Voo, R., Fang, W., Wang, Z., Suk, D.W. & Peacor, D.R., 1993. Palaeomagnetism and electron microscopy of the Emeishan Basalts, Yunnan, China, *Tectonophysics,* **221,** 367–379.

Watson, G.S. & Enkin, R.J., 1993. The fold test in palaeomagnetism as a parameter estimation problem, *Geophys. Res. Lett.,* **20,** 2135–2137.

Well, R.E. & Coe, R.S., 1985. Palaeomagnetism and geology of Eocene

volcanic rocks of southwest Washington: Implications for mechanisms of rotation, *J. geophys. Res.,* **90,** 1925–1947.

Xu, J., 1980. Horizontal displacement along the Tancheng-Lujiang fault zone and its geological significance, in *Scientific Papers on Geology for International Exchange,* pp. 129–142, Geological Publishing House, Beijing.

Zhao, X. *et al*., 1999. Clockwise rotation recorded in Early Cretaceous rocks of South Korea: implications for tectonic affinity between the Korean Peninsula and North China, *Geophys. J. Int.,* **139,** 447–463.

Zijderveld, J.D.A., 1967. AC demagnetisation of rocks: Analysis of results, in *Method in Palaeomagnetism,* pp. 254–286, eds Collinson, D.W., Creer, K.M. & Runcorn, S.K., Elsevier, Amsterdam.